Acta Crystallographica Section A
**Foundations of Crystallography**
ISSN 0108-7673

Received 16 July 2003
Accepted 30 September 2003



# Crystallography of a new metastable phase in Zr–N alloy

**P. Li[a]* and J. M. Howe[b]**

[a]Center for Solid State Science, Arizona State University, Tempe, AZ 85287-1704, USA, and [b]Department of Materials Science and Engineering, University of Virginia, Charlottesville, VA 22904-4745, USA. Correspondence e-mail: pengli@asu.edu

Selected-area and convergent-beam electron diffraction were used to determine the lattice, point and space groups of a new metastable phase (designated the $\pi$ phase) in the Zr–N system. The $\pi$ phase has a body-centered tetragonal lattice with $a \simeq 0.66$ nm and a $c/a$ ratio of 0.81. The point-group symmetry of the phase is $4/mmm$ and the space group is $I4/mmm$.

## 1. Introduction

Ordered phases in the Ti–N system have been studied in detail (Gusev & Rempel, 1993, 1997). For example, an ordered tetragonal $Ti_2N$ phase ($M_2X$ type) with space group $I4_1/amd$ has been experimentally observed by many investigators (Christensen *et al.*, 1985; Nagakura & Kusunoki, 1977). In the Zr–N system, a metastable phase ($Zr_4N$) with a monoclinic crystal structure has been found by Sharma *et al.* (2003). In our recent study of Zr–N alloys, another new metastable phase was identified. The crystal lattice, point group and space group of this new phase are given in this paper.

## 2. Experimental procedures

### 2.1. Sample preparation

The sample used in this study was made by encapsulating a 50 μm-thick foil of high-purity $\alpha$-Zr in a sealed quartz tube under an atmosphere of high-purity N and nitriding for 2 h at 1473 K. The N content of the foil was determined to be 34.1 at.% by the increase in weight of the nitrided specimen compared to the initial high-purity Zr foil. To produce a homogeneous distribution of N throughout the foil, it was subsequently annealed for 10 h at 1473 K in an encapsulated tube filled with high-purity Ar and then quenched into cold water.

Discs 3 mm in diameter were cut from the foil using an ultrasonic cutter. A double-jet technique was then used to electrolytically thin the discs. An electrolyte of perchloric acid and methanol in the ratio 3:97 by volume was used, and the disc specimens were thinned at 18 V and −223 K. Final thinning was performed by $Ar^+$ ion-beam milling for 1 h at liquid-nitrogen temperature in a Gatan Model 600 DuoMill™.

### 2.2. Transmission electron microscopy

The thinned specimen was examined in a JEOL 2000FXII transmission electron microscope (TEM) at 200 kV. The specimen was tilted along different Kikuchi bands to reach several low-index zone axes and the corresponding selected-area diffraction patterns (SADPs) were then recorded. *Desktop Microscopist*™ software was used to analyze SADPs and Kikuchi maps in order to determine the zone axes of the SADPs for the unknown phase. The specimen was then transferred to a JEOL 2010 F TEM operating at 200 kV to perform convergent-beam electron diffraction (CBED) analyses. The phase of interest was oriented along its fourfold axis and CBED patterns were obtained at both low and high camera lengths, using both small and large condenser apertures, to capture all of the symmetry features available in the patterns. Final adjustment of the phase orientation was performed using the dark-field tilt controls on the microscope and fine adjustment of the convergence angle was performed using the $\alpha$-selector control.

## 3. Results

### 3.1. Bravais-lattice determination

A new phase (designated the $\pi$ phase) was occasionally observed in Zr–N alloys containing approximately 34 at.% N. An example of the phase is shown in Fig. 1. The composition of the phase has not yet been determined because of the difficulties encountered in quantifying the N content owing to the low scattering cross section of N and the strongly absorbing Zr atoms (Sharma *et al.*, 2003). SADPs from four different zone axes in the $\pi$ phase are shown in Fig. 2. As demonstrated in Fig. 3, the crystal contains a fourfold axis. Therefore, the crystal is either tetragonal or cubic. The SADPs in Fig. 2 have been indexed with the fourfold axis along the $z$ direction. From the $[1\bar{1}1]$ diffraction pattern in Fig. 2($c$), it can be seen that $|\mathbf{g}_{011}| = |\mathbf{g}_{\bar{1}01}| \neq |\mathbf{g}_{110}|$, which means that the crystal is tetragonal. It can readily be shown that:

$$(a/c)^2 = 2(|g_{110}|/|g_{011}|)^2 - 1,$$

so the $c/a$ ratio of the $\pi$ phase can be calculated from Fig. 2($c$). The measured value of $|\mathbf{g}_{110}|/|\mathbf{g}_{011}|$ is 0.89, which gives a $c/a$ ratio of 0.81. The unknown lattice parameters (*i.e.* $a$ and $c$) of

the $\pi$ phase can be approximately calculated from Fig. 2(*a*), using the diffraction pattern of the $\alpha$-Zr (hexagonal close-packed crystal structure with $a_{Zr} = 0.32$ nm and $c_{Zr} = 0.52$ nm) as a reference. The calculated values are $a = 0.66$ and $c = 0.53$ nm, where $a \approx 2a_{Zr}$ and $c \approx c_{Zr}$.

A tetragonal Bravais lattice can be either primitive or body-centered. Comparison between the positions of the diffraction spots in the first-order Laue zone (FOLZ) with those in the zero-order Laue zone (ZOLZ) can be used to determine the centering of the unit cell (Buxton *et al.*, 1976). Fig. 3 shows a CBED pattern including both the FOLZ and ZOLZ diffractions, obtained along the [001] zone axis from the $\pi$ phase. In Fig. 3, the FOLZ diffractions are displaced and appear halfway between the ZOLZ diffractions along two orthogonal directions, as indicated by the lines in the figure. This result indicates that the tetragonal Bravais lattice of the $\pi$ phase is body-centered and not primitive.

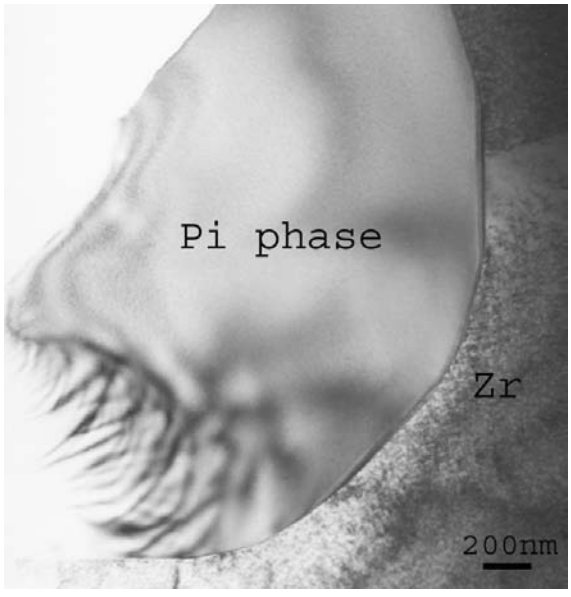


**Figure 1**
Bright-field TEM image of the $\pi$ phase in the Zr matrix.

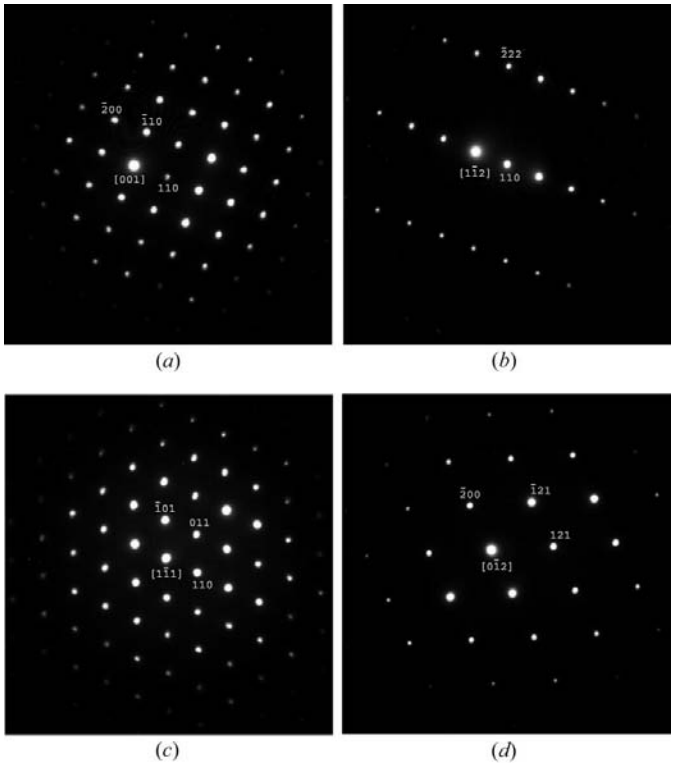


**Figure 2**
SADPs of the $\pi$ phase along: (*a*) [001], (*b*) [1$\bar{1}$2], (*c*) [1$\bar{1}$1] and (*d*) [1$\bar{1}$2] zone axes.

### 3.2. Point-group determination

Both the whole pattern (WP) and bright-field (BF) discs in the ZOLZ in Fig. 4(*a*) display 4*mm* symmetry. That is, they possess fourfold rotational symmetry about an axis that lies in the center of the BF disc (indicated by an asterisk in Fig. 4*a*), parallel to the electron-beam direction and they display two mirror lines 45° apart, as indicated in Fig. 4(*a*). The FOLZ in Fig. 4(*b*) also displays 4*mm* symmetry, giving additional confirmation to a WP symmetry of 4*mm*. According to Fultz & Howe (2001) and Buxton *et al.* (1976), the only two diffraction groups in which both the BF disc and WP display 4*mm* symmetry are 4*mm* and $4mm1_R$.

To further distinguish between these two diffraction groups, the CBED method developed by Tanaka & Terauchi (1985) was employed. Their method uses the detail within one or a pair of symmetric many-beam (SMB) patterns to obtain the diffraction group. Fig. 4(*c*) shows an exact [001] zone-axis pattern, which displays 4*mm* symmetry. In Fig. 4(*d*), the incident beam was tilted so the $\bar{1}\bar{1}0$ disc is centered on the optic axis to form a SMB pattern. Inspection of the symmetries within the surrounding discs shows that the $\bar{2}\bar{2}0$ disc has 2*mm* symmetry (note that there are only weak intensity variations

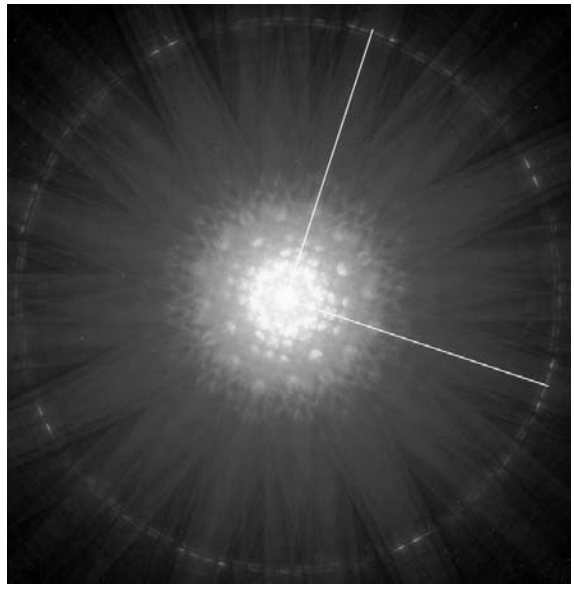

**Figure 3**
FOLZ and ZOLZ diffractions obtained from the $\pi$ phase in a [001] orientation.

in the disc and HOLZ interactions are weak in the SMB pattern, so that this symmetry determination must be considered with caution), while all the other discs display mirror lines that intersect the center of the $\bar{2}\bar{2}0$ disc. This pattern symmetry corresponds to that of the diffraction group $4mm1_R$ (Tanaka, Saito & Sekii, 1983; Tanaka & Terauchi, 1985).

Having determined the diffraction group of the $\pi$ phase from the CBED pattern symmetries, the next step is to find the crystal point group. According to Buxton *et al.* (1976), the point groups $4/mmm$ and $m3m$ are the only ones that correspond to a diffraction-group symmetry of $4mm1_R$. However, since the Bravais lattice of this phase was previously determined to be body-centered tetragonal, it is possible to eliminate $m3m$, since this is cubic. In conclusion, the point group of the $\pi$ phase is $4/mmm$.

### 3.3. Space-group determination

There are 20 space groups corresponding to the point group $4/mmm$. Only four of these have a body-centered lattice, *i.e.* $I4/mmm$ (No. 139), $I4/mcm$ (No. 140), $I4_1/amd$ (No. 141) and $I4_1/acd$ (No. 142) (Henry & Lonsdale, 1969; Tanaka, Sekii & Nagasawa, 1983; Tanaka & Terauchi, 1985). There is no systematic extinction for any diffraction discs in the [001] zone axis for space group Nos. 139 and 140, while there are special

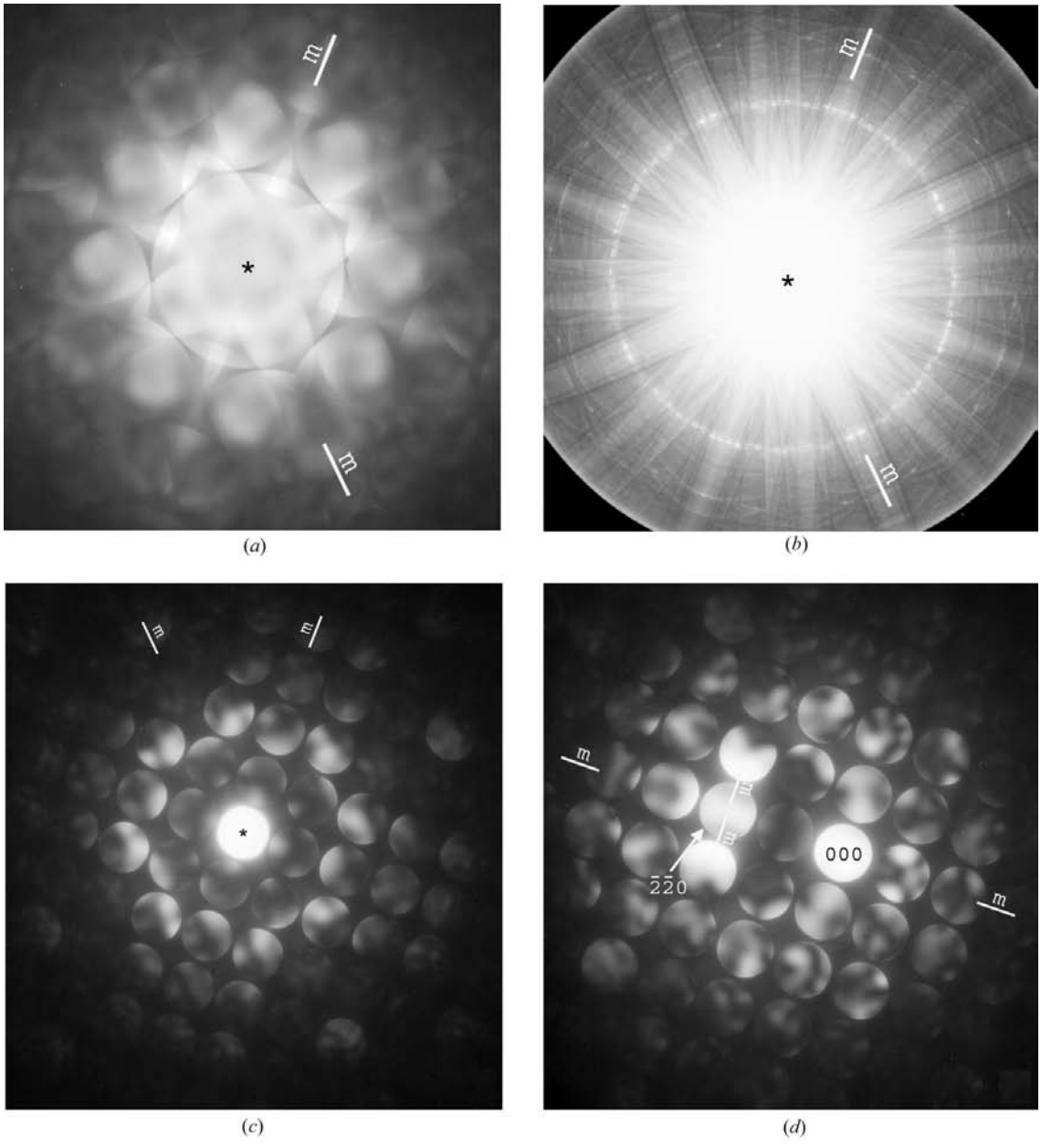


**Figure 4**
CBED patterns obtained from the $\pi$ phase in a [001] orientation: (*a*) BF disc and WP symmetry; (*b*) WP symmetry including FOLZ; (*c*) ZOLZ zone-axis pattern; and (*d*) SMB pattern obtained with the optic axis centered on the $\bar{1}10$ disc.

extinctions because of the diamond glide plane in space group Nos. 141 and 142. In this case, Gjønnes–Moodie (G–M) lines (Gjønnes & Moodie, 1965) should be present in the $hh0$ and $\bar{h}h0$ diffraction discs in the [001] zone axis. Such G–M lines are definitely not present in the 110 and $\bar{1}10$ diffraction discs in Figs. 4(*c*) and (*d*), indicating that possible space groups for the $\pi$ phase are $I4/mmm$ (No. 139) or $I4/mcm$ (No. 140). For these two possible space groups, the general condition that $k, l = 2n$ for $0kl$ reflections applies to space group $I4/mcm$, but not to $I4/mmm$ (Henry & Lonsdale, 1969). Although no CBED patterns were taken along the $[1\bar{1}1]$ zone axis in Fig. 2(*c*), the presence of strong 011 diffraction spots indicates that these reflections are allowed. Therefore, there appear to be no systematic extinctions beyond the body center, indicating that the space group of the $\pi$ phase is $I4/mmm$ (No. 139).

## 4. Conclusions

A new metastable phase (designated the $\pi$ phase) was found in the Zr–N system. This phase is body-centered tetragonal with a space-group symmetry of $I4/mmm$ (No. 139). The $c/a$ ratio of the $\pi$ phase is approximately 0.81 with calculated values $a = 0.66$ and $c = 0.53$ nm.

This research was supported by the National Science Foundation under grant DMR-9908855. The authors also thank Professors W. A. Jesser and G. J. Shiflet for use of their encapsulating equipment.

## References

Buxton, B. F., Eades, J. A., Steeds, J. W. & Rackham, G. M. (1976). *Philos. Trans. R. Soc. London Ser. A*, **281**, 171–194.
Christensen, A. N., Alamo, A. & Landesman, J. P. (1985). *Acta Cryst.* C**41**, 1009–1011.
Fultz, B. & Howe, J. M. (2001). *Transmission Electron Microscopy and Diffractometry of Materials*, pp. 275–331. New York: Springer.
Gjønnes, J. & Moodie, A. F. (1965). *Acta Cryst.* **19**, 65–67.
Gusev, A. I. & Rempel, A. A. (1993). *Phys. Status Solidi A*, **135**, 15–58.
Gusev, A. I. & Rempel, A. A. (1997). *Phys. Status Solidi A*, **163**, 273–304.
Henry, N. F. M. & Lonsdale, K. (1969). Editors. *International Tables for X-ray Crystallography*, Vol. I. Birmingham: Kynock Press.
Nagakura, S. & Kusunoki, T. (1977). *J. Appl. Cryst.* **10**, 52–56.
Sharma, S., Moore, K. T. & Howe, J. M. (2003). *Philos. Mag.* **83**, 31–51.
Tanaka, M., Saito, R. & Sekii, H. (1983). *Acta Cryst.* A**39**, 357–368.
Tanaka, M., Sekii, H. & Nagasawa, T. (1983). *Acta Cryst.* A**39**, 825–837.
Tanaka, M. & Terauchi, M. (1985). *Convergent-Beam Electron Diffraction.* Tokyo: JEOL Ltd.